INSIGHTS INTO THE INFLUENCE OF SNOW MICROSTRUCTURE ON THE COMPRESSIVE STRENGTH OF WEAK LAYERS

Jakob Schöttner[1,*], Melin Walet[1], Philipp Rosendahl[2], Philipp Weißgraeber[3], Valentin Adam[1,2], Florian Rheinschmidt[2], Benjamin Walter[1], Jürg Schweizer[1], Alec van Herwijnen[1]

[1] *WSL Institute for Snow and Avalanche Research SLF, Flüelastrasse 11, CH - 7260 Davos Dorf*
[2] *Institute for Structural Mechanics and Design, TU Darmstadt, Franziska-Braun-Str. 3, D - 64287 Darmstad*
[3] *Chair of Lightweight Design, University of Rostock, Albert-Einstein-Str. 2, D - 18059 Rostock*

ABSTRACT: Natural weak layers exhibit a variety of different microstructures and densities, and thus show different mechanical behavior. Up to now, mechanical properties of snow have been mainly evaluated based on bulk proxies such as snow density, not accounting for relevant microstructural characteristics. To establish a link between the microstructure of weak layers and their mechanical properties, we tested weak layers of three different categories (faceted crystals and depth hoar, decomposed particles and rounded grains, and buried surface hoar) in displacement-controlled laboratory experiments using a uniaxial testing machine and recorded their microstructure using micro-computed tomography (μCT) imaging. The compressive strength of 295 tested samples covered three orders of magnitude (0.5 kPa to 1 MPa) for weak layer densities ranging from 65 kg m^{-3} to 470 kg m^{-3}. As expected, our results show a strong correlation between weak layer density and strength. At the same time, we observe distinct scaling of different types of weak layers with density, highlighting the importance of snow microstructure for mechanical considerations. These results will help us to establish a link between density, microstructural properties and strength of weak snow layers, which is needed for the next generation of snow cover and avalanche release models.

Keywords: snow slab avalanches, snow mechanics, weak snow layers, strength, microstructure

1. INTRODUCTION

Dry-snow slab avalanches are responsible for the majority of avalanche fatalities, which makes them most relevant for avalanche forecasting (e.g. Schweizer and Jamieson, 2001). This type of avalanche requires a weak layer within the snowpack. If this weak layer fails e.g. due to the impact of a skier, this failure may propagate across the slope and the avalanche releases (e.g. Schweizer et al., 2016). Most weak layers form as a result of high rates of water vapor transport within the snowpack or from the atmosphere, or as a result of precipitation events.

Natural weak layers exhibit a variety of different microstructures and densities, and thus show different mechanical behavior (e.g. Jamieson and Johnston, 2001). Up to now, mechanical properties of snow have been mainly evaluated based on bulk proxies such as snow density. This does not account for relevant microstructural characteristics, although snow properties can vary by orders of magnitude for identical densities depending on the microstructure (e.g. Shapiro et al., 1997; Mellor, 1975).

To establish a link between weak layer strength and microstructure, we performed displacement-controlled compression experiments on weak layers with a wide range of microstructural morphologies and recorded the microstructure of every batch of samples using μCT imaging (e.g. Coléou et al., 2001). In order to test a wide range of microstructures we used both natural and artificially grown weak layers. To quantify the influence of snow microstructure, we tested weak layers of three different categories: faceted crystals and depth hoar, decomposed particles and rounded grains, and buried surface hoar. This study is a first step to quantify the influence of snow microstructure on the strength under multiaxial loading conditions, which is needed for the next generation of snow cover and avalanche release models.

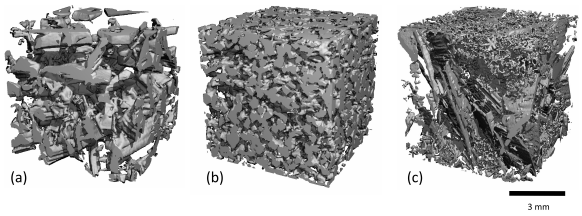

Figure 1: Exemplary microstructures obtained from μCT images for each tested category of weak layers: (a) faceted crystals and depth hoar, (b) decomposed particles and rounded grains and (c) buried surface hoar.

2. METHODS

In order to evaluate the influence of microstructure on the strength of weak layers, a comprehensive

*Corresponding author address:
Jakob Schöttner
WSL Institute for Snow and Avalanche Research SLF
Flüelastrasse 11, CH - 7260 Davos Dorf
Email: jakob.schoettner@slf.ch

dataset with a wide range of microstructural morphologies is required. Since we lack a biaxial testing machine (we show the current development of two machines in Schöttner et al., 2024), for the time being, we performed compression experiments on different types of weak layers with a wide range of microstructures. To capture the microstructure, we used μCT imaging (e.g. Calonne et al., 2020; Proksch et al., 2016).

To perform mechanical experiments, the weak layers need to be contained between dense snow layers. This allows us to cut and transport the samples without damaging the weak layer and provides an interface for the mechanical tests. This sandwich-like configuration also helps to localize the failure within the weak layer and is therefore required for experimental testing of any type of weak layer. We always produced or harvested a block of snow ("parent sample") (300 mm $\times$ 400 mm) containing a weak layer, from which we cut 5 specimens for the mechanical experiments (65 mm $\times$ 140 mm) and one specimen for the μCT scan.

In order to quantify the effect of microstructure, we used weak layers of three different types: faceted crystals and depth hoar, decomposed particles and rounded grains, and buried surface hoar. Examples of the corresponding microstructures are shown in Figure 1. For the first two types it would be very time consuming to find natural samples with different microstructures in a sandwich-like configuration for mechanical testing. We have therefore grown these weak layers artificially in the cold laboratory. Surface hoar, on the other hand, often forms near open water in winter. This makes it easier to collect natural samples instead of growing them artificially.

2.1 Artificially grown weak layers

To grow artificial depth hoar weak layers we sieved artificially produced snow (Schleef et al., 2014) in between two dense snow slabs and subjected this sandwich to a temperature gradient for a prolonged time (e.g. Capelli et al., 2018; Fukuzawa and Narita, 1993). The dense slabs were made from compacted snow consisting of decomposed particles or rounded grains. Depending on the type of snow, the sieve mesh size, temperature and the duration of metamorphism, it was possible to obtain samples with a wide range of densities and microstructures. However, the density of the weak layer was limited by the required higher density of the slabs. To achieve weak layer densities above 350 kg m^{-3}, we used slabs of compacted wet snow. In this way we were able to achieve weak layer densities up to 470 kg m^{-3}.

For rounded grains we used a similar procedure of sample preparation. Since we found that the upper dense slab sometimes was poorly bonded to the weak layer, we sieved the second dense slab directly onto the weak layers rather than using compacted snow. The sandwich structures were then stored for up to 6 months at -5 °C to -20 °C.

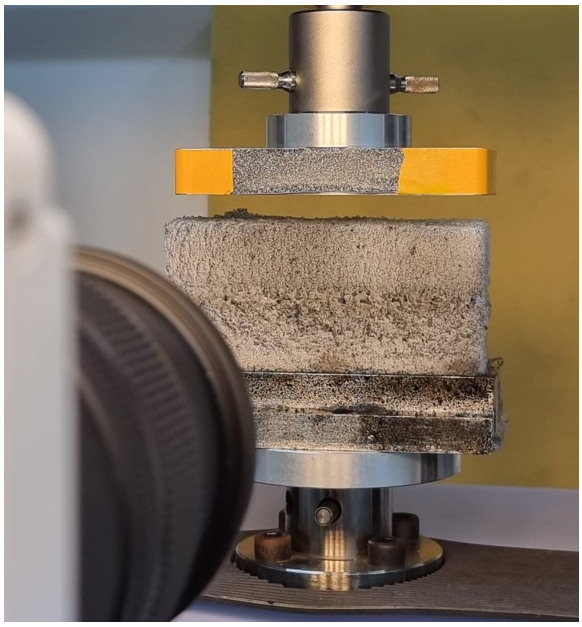

Figure 2: Experimental setup of the compression experiments. The samples are sprayed with black ink to increase the contrast for the high speed video recording.

2.2 Natural weak layers

We sampled three different surface hoar events in the winter of 2023/24 near a shaded creek (1650 m ASL) in Davos (Switzerland). Since we found that manually covering surface hoar by sieving new snow was more damaging to the crystals than a natural snowfall, we sampled only surface hoar layers that had already been covered by natural snow. Depending on the density and thickness of the natural new snow layer, we sieved an additional layer of dense snow on top of it, in order to have a stable and dense interface for the mechanical experiments.

2.3 Mechanical testing

We used a uniaxial testing machine in combination with a 10 kN load cell to perform the displacement-controlled compression experiments (see Figure 2). The displacement rate of the machine was set to reach a strain rate of 10^{-2} s^{-1} in the weak layer, however, since we also observed deformation at the top surface of the sample, the effective loading rate in the weak layer was likely lower. From the resulting stress signal (an example is shown in Figure 4) it was straight forward to determine the ultimate strength. In most experiments, we also observed pop-ins prior to failure due to collapse processes from the snow-machine interface.

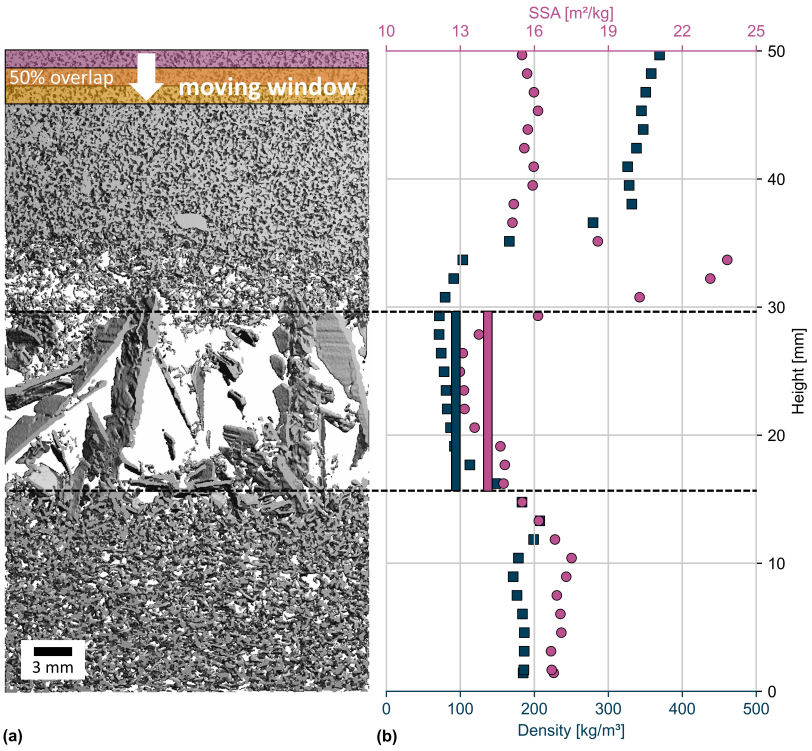

Figure 3: Comparison of the bulk μCT evaluation and the moving window analysis. (a) shows a vertical cross-section through the μCT scan of a natural buried surface hoar weak layer and the size and overlap of the moving window. The dashed lines are the manually selected extent of the weak layer. (b) shows a representative example comparison of the moving window analysis and the bulk measurements (representing weak layer averages, shown as vertical bars) for density (black squares) and specific surface area (SSA) (purple circles). For the moving window analysis we used a window size of 1000 $\times$ 1000 voxel, a window height of 100 voxel and a vertical overlap of 50%.

2.4 Microstructure quantification

The microstructure of each parent sample (5 specimens) was analyzed using μCT imaging. The reconstructed image was Gaussian filtered to reduce noise (width = 1.2 voxels, support = 2 voxels) and binary segmented (Hagenmuller et al., 2013). The average weak layer density ρ° was calculated from the volume fraction of the segmented binary μCT image (Calonne et al., 2020; Proksch et al., 2016) and the density of ice ($\rho^{\bullet}$ = 917 kg m^{-3}). The binarized image was also used to calculate the vertical anisotropy A^{CT} of the weak layer using the ratio of the exponential correlation lengths p_{ex}. SSA was calculated from the triangulated surface of the binary image which was normalized with the ice mass (Calonne et al., 2020; Schleef and Löwe, 2013).

In addition to these bulk evaluations, which represent averages of the entire weak layer, we also performed a moving window analysis to obtain profiles of density and specific surface area (SSA) over the height of the weak layer. Since compressive strength depends strongly on snow density, our hypothesis is that the minimum density obtained by moving window analysis could shed light on the failure location within the weak layer (e.g. Hagenmuller et al., 2014). An example profile of density and SSA is shown in Figure 3.

For the μCT scans we used sample holders with diameters of 50 mm, 70 mm and 90 mm depending on how fragile the weak layers were, yielding an effective resolution (voxel size) of (16.2 μm)^3, (22.8 μm)^3, and (29.1 μm)^3, respectively. We then selected a region of interest (ROI) only containing the weak layer. The size of the ROI was limited by either the thickness of the weak layer or the size of the sample holder.

3. RESULTS

The compressive strength of 295 tested samples covered three orders of magnitude (0.5 kPa to 1 MPa) for weak layer densities ranging from 65 kg m^{-3} to 470 kg m^{-3} and is summarized in Table 1. As expected, our results show a strong correlation between weak layer density and compressive strength. Also, we observe a different scaling of the compressive strength with density for different weak layer types.

To show the scaling of compressive strength and density, we fit a power law to our normalized data. For the compressive strength $\sigma_{\mathrm{c}}^{\circ}$ we used the yield strength $\sigma_{\mathrm{y}}^{\bullet} \approx 2$ MPa of polycrystalline ice (e.g. Petrovic, 2003; Haynes, 1978) for the normalization. We normalized the density ρ° of our weak layers to the density of ice ($\rho^{\bullet}$ = 917 kg m^{-3}). To fit the power

	Number of samples	Density range [kg m^{-3}]	Strength range [kPa]	a	b	χ^2_ν
Faceted crystals and depth hoar	118	150 - 470	0.5 - 1000	15	5.5	2.3
Decomposed particles and rounded grains	124	120 - 360	1.0 - 60	13×10^{-2}	2.5	3.4
Surface hoar	53	65 - 175	0.5 - 10	90×10^{-3}	2.0	1.4

Table 1: Preliminary results for the compressive strength of the three types of weak layers. The coefficients a and b are the fitting parameters of the power law given in Eq. 1. The value χ^2_ν evaluates the goodness of the fit, normalized by the degrees of freedom (values closer to 1 are better).

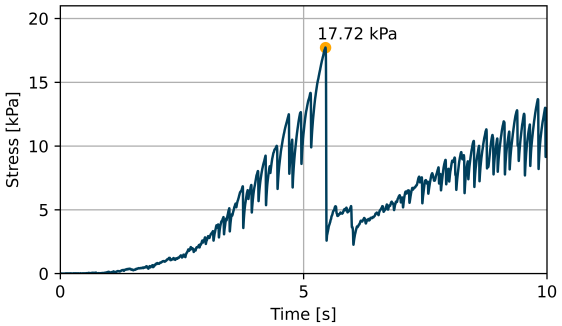

Figure 4: Example stress signal obtained from a compression experiment. The round marker highlights the point of ultimate strength, the smaller peaks are pop-ins from local failures at the sample surface (before the failure) or due to crushing within the weak layer (after the failure).

law (Eq. 1), we used an orthogonal distance regression (ODR - Boggs and Rogers (1990)).

$$\frac{\sigma_c^\circ}{\sigma_y^\bullet} = a\left(\frac{\rho^\circ}{\rho^\bullet}\right)^b \tag{1}$$

Our data have measurement uncertainties both in terms of density and in terms of strength. For the strength we take the average of the 5 compression experiments per parent sample and the corresponding standard deviation. For the average density the error is composed of the measurement error of the μCT (about 1% according to Freitag et al. (2004) and the expected variations within a parent sample. We found this variation to be about 17 kg m^{-3}, by calculating the mean daily difference between two independently but identically produced depth hoar parent samples over the duration of one week (12 scans in total).

For the artificially grown depth hoar the compressive strength of 118 samples was in the range of 0.5 kPa to 1 MPa for densities between 150 kg m^{-3} and 470 kg m^{-3}. We found that the relation between the normalized weak layer density and normalized compressive strength was best described by a power law with an exponent of 5.5 (variable b in Eq. 1).

The natural surface hoar layers collected close to a creek (53 samples in total) had densities between 65 kg m^{-3} and 175 kg m^{-3}. Their compressive strength was in the range of 0.5 kPa to 10 kPa and was best described by a power law with an exponent of 2.5.

Weak layers consisting of rounded grains showed more scatter in the data than the other two grain types. 124 samples of this type with densities between 120 kg m^{-3} and 360 kg m^{-3} showed compressive strengths between 1 kPa and 60 kPa. The scaling of normalized compressive strength with normalized density followed a power law with an exponent of 2.0.

4. DISCUSSION

Although we are interested in the influence of microstructure for a wide range of mixed-mode loading conditions, we chose to use only compressive strength as a first step because the corresponding experiments are straightforward and failed experiments are easy to recognize.

Our results indicate a difference in the scaling of the compressive strength of weak layers with density. While the power law exponents of the normalized data for surface hoar and rounded grains are similar (2.0 - 2.5), we observe an exponent of 5.5 for weak layers consisting of depth hoar. This suggests that different failure mechanisms are at work for depth hoar than for other types of weak layers (Gibson and Ashby, 1997). As the strength of snow is governed by the bonds between grains, this could indicate an increase in bond size and number for depth hoar, or a reduction in the mechanically relevant length scales within the material. Overall, at higher densities, a greater proportion of the material in the depth hoar contributes to its strength.

Buried surface hoar shows similar behavior as rounded grains. This suggests that weak layers of buried surface hoar are not particularly 'fragile' compared to rounded grains under compression, but that this is the only crystal configuration that can persist at such low densities within the snowpack.

The reported power law fits and χ^2_ν values are strongly dependent on the estimated measurement errors. For the density, we used the combined error of the measurement accuracy (1%) of the μCT and

the variability within a parent sample. However, it is difficult to obtain an objective estimate for this variability, and so far we have only estimated a value for artificially grown weak layers of depth hoar. A next step will be to refine this error estimate and also investigate the variability of the other types of weak layers. This will likely affect our reported power law fits and χ^2 values.

5. CONCLUSION AND OUTLOOK

In this study, we collected a large dataset of compressive strength and microstructure for different types of weak layers, which allows us to draw some preliminary conclusions about the influence of snow microstructure on mechanical properties. We found that different types of weak layers show different scaling of the compressive strength with density. By fitting a power law to the normalized data we found the exponent to be 5.5 for faceted crystals and depth hoar, 2.5 for decomposed particles and rounded grains, and 2.0 for surface hoar. This suggests that microstructure plays an important role in mechanical considerations of snow, and that the compressive strength of depth hoar may have different scaling mechanisms with density compared to other types of snow.

In the future, we will extend our experiments to test the strength of weak layers under multiaxial loading conditions. The scaling of strength and microstructure under these conditions will give us valuable information about the failure processes and open up ways of abstracting the microstructure to simplify mechanical modelling, which will ultimately be needed for the next generation of snow cover and avalanche release models.

REFERENCES

Boggs, P. T. and Rogers, J. E.: Orthogonal distance regression, Contemporary Mathematics, 112, 183–194, 1990.

Calonne, N., Richter, B., Löwe, H., Cetti, C., ter Schure, J., Van Herwijnen, A., Fierz, C., Jaggi, M., and Schneebeli, M.: The RHOSSA campaign: multi-resolution monitoring of the seasonal evolution of the structure and mechanical stability of an alpine snowpack, The Cryosphere, 14, 1829–1848, https://doi.org/10.5194/tc-14-1829-2020, 2020.

Capelli, A., Reiweger, I., and Schweizer, J.: Acoustic emission signatures prior to snow failure, Journal of Glaciology, 64, 543–554, https://doi.org/10.1017/jog.2018.43, 2018.

Coléou, C., Lesaffre, B., Brzoska, J. B., Ludwig, W., and Boller, E.: Three-dimensional snow images by X-ray microtomography, Annals of Glaciology, 32, 75–81, https://doi.org/10.3189/172756401781819418, 2001.

Freitag, J., Wilhelms, F., and Kipfstuhl, S.: Microstructure-dependent densification of polar firn derived from X-ray microtomography, Journal of Glaciology, 50, 243–250, https://doi.org/10.3189/172756504781830123, 2004.

Fukuzawa, T. and Narita, H.: An experimental study on the mechanical behavior of a depth hoar layer under shear stress, in: Proceedings ISSW 1992. International Snow Science Workshop, 4-8 October 1992, pp. 171–175, Breckenridge, Colorado, USA, 1993.

Gibson, L. J. and Ashby, M. F.: Cellular Solids, Cambridge University Press, https://doi.org/10.1017/CBO9781139878326, 1997.

Hagenmuller, P., Chambon, G., Lesaffre, B., Flin, F., and Naaim, M.: Energy-based binary segmentation of snow microtomographic images, Journal of Glaciology, 59, 859–873, https://doi.org/10.3189/2013JoG13J035, 2013.

Hagenmuller, P., Calonne, N., Chambon, G., Flin, F., Geindreau, C., and Naaim, M.: Characterization of the snow microstructural bonding system through the minimum cut density, Cold Regions Science and Technology, 108, 72–79, https://doi.org/10.1016/j.coldregions.2014.09.002, 2014.

Haynes, F. D.: Effect of temperature on the strength of snow-ice, Tech. rep., " Department of the Army, Cold Regions Research and Engineering Laboratory, Corps of Engineers, CRREL Report 78-27, Hanover, New Hampshire, 1978.

Jamieson, B. and Johnston, C. D.: Evaluation of the shear frame test for weak snowpack layers, Annals of Glaciology, 32, 59–69, https://doi.org/10.3189/172756401781819472, 2001.

Mellor, M.: A review of basic snow mechanics, in: Symposium at Grindelwald 1974 - Snow Mechanics, IAHS Publ., 114, pp. 251–291, 1975.

Petrovic, J. J.: Mechanical properties of ice and snow, Journal of Materials Science, 38, 1–6, https://doi.org/http://dx.doi.org/10.1023/A:1021134128038, 2003.

Proksch, M., Rutter, N., Fierz, C., and Schneebeli, M.: Intercomparison of snow density measurements: bias, precision, and vertical resolution, The Cryosphere, 10, 371–384, https://doi.org/10.5194/tc-10-371-2016, 2016.

Schleef, S. and Löwe, H.: X-ray microtomography analysis of isothermal densification of new snow under external mechanical stress, Journal of Glaciology, 59, 233–243, https://doi.org/10.3189/2013JoG12J076, 2013.

Schleef, S., Jaggi, M., Löwe, H., and Schneebeli, M.: An improved machine to produce nature-identical snow in the laboratory, Journal of Glaciology, 60, 94–102, https://doi.org/10.3189/2014JoG13J118, 2014.

Schöttner, J., Walet, M., Marques, E., Carbas, R., Adam, V., Hohl, M., Weißgraeber Philipp, Rosendahl, P., Kraus, S., Rheinschmidt, F., Hedvard, M., da Silva, L. F. M., Schweizer, J., and van Herwijnen, A.: Developing two multiaxial testing machines to link strength and microstructure of weak snow layers, International Snow Science Workshop Proceedings 2024, Tromsø, Norway, 2024.

Schweizer, J. and Jamieson, J.: Snow cover properties for skier triggering of avalanches, Cold Regions Science and Technology, 33, 207–221, https://doi.org/10.1016/S0165-232X(01)00039-8, 2001.

Schweizer, J., Reuter, B., Van Herwijnen, A., and Gaume, J.: Avalanche Release 101, Proceedings ISSW 2016, International Snow Science Workshop, Breckenridge CO, U.S.A., 3-7 October 2016, pp. 1–11, 2016.

Shapiro, L., Johnson, J., Sturm, M., and Blaisdell, G.: Snow Mechanics: Review of the State of Knowledge and Applications, Tech. rep., US Army Corpsof Engineers Cold Regions Research and Engineering Laborator, 1997.